

# Observation of two-dimensional lattice vector solitons

Zhigang Chen, Anna Bezryadina, and Igor Makasyuk

Department of Physics and Astronomy, San Francisco State University, San Francisco, California 94132, and  
TEDA Applied Physics School, Nankai University, Tianjin, China

Jianke Yang

Department of Mathematics and Statistics, University of Vermont, Burlington, Vermont 05401

Received January 27, 2004

We demonstrate the formation of fundamental and dipolelike vector solitons in an optically induced two-dimensional photonic lattice. Such vector solitons are realized by mutual trapping of two beams in the lattice. Our theoretical results are in good agreement with experimental observations. © 2004 Optical Society of America

OCIS codes: 270.5530, 190.4420.

Discrete solitons (DSs) and intrinsic localized states in periodic structures have attracted considerable interest in optics,<sup>1,2</sup> not only because of their potential applications but also because such phenomena also exist in a variety of other discrete nonlinear systems. Recently, a series of experiments demonstrated the formation of DSs in fabricated semiconductor waveguide arrays<sup>3,4</sup> and in optically induced photonic lattices.<sup>5–9</sup> Several exciting theoretical predictions about DSs were made as well, including discrete vortex solitons<sup>10,11</sup> and discrete vector solitons.<sup>12–14</sup> Among such self-localized states, discrete vector solitons make up an important family. Although vector solitons have been realized previously in continuum nonlinear systems, they were observed only recently in a discrete system of one-dimensional AlGaAs waveguide arrays.<sup>15</sup>

In this Letter we report the experimental observation and numerical modeling of two-dimensional (2D) discrete vector solitons in an optically induced photonic lattice. We demonstrate that two mutually incoherent beams can lock into a fundamental vector soliton while propagating along the same lattice site, although each beam alone would experience discrete diffraction under the same conditions. When the two beams are launched in parallel into two neighboring lattice sites, they can also form a localized state akin to a dipole vector soliton.

The experiments were performed in a biased photorefractive crystal illuminated by a laser beam ( $\lambda = 488$  nm) passing through a rotating diffuser and an amplitude mask as shown in Fig. 1. The photorefractive crystal (SBN:60, 5 mm  $\times$  5 mm  $\times$  8 mm) provides a self-focusing noninstantaneous nonlinearity. The amplitude mask provides spatial modulation after the diffruser on the otherwise uniform beam, which exhibits a pixellike intensity pattern at the input face of the crystal.<sup>16</sup> This pixellike beam is ordinarily polarized and is partially coherent as controlled by the rotating diffruser, forming a stable and nearly invariant waveguide lattice in the crystal. A Gaussian beam split from the same laser output is sent into a Mach–Zehnder interferometer. The two extraordinarily polarized beams exiting from the interferometer are combined with the

lattice beam, propagating collinearly through the crystal. When a piezoelectric-transducer mirror is ramped at a fast frequency, the two beams for the vector components are realized—each beam itself is coherent and experiences a strong self-focusing nonlinearity but is mutually incoherent with the other. The two components are monitored separately with a CCD camera, taking advantage of the noninstantaneous response of the crystal.<sup>17</sup> In addition, a uniform incoherent beam is used as background illumination for fine tuning the nonlinearity.

Typical experimental results of a 2D discrete vector soliton are presented in the first two rows of Fig. 2, which were obtained with a square lattice of 20- $\mu$ m nearest-neighbor spacing. The two mutually incoherent beams [Fig. 2(a), rows 1 and 2] were launched into the same lattice site, with a combined peak intensity approximately six times weaker than that of the lattice beam. Discrete diffraction of each beam was observed at a low bias field of 100 V/mm [Fig. 2(b)], but the two beams formed a coupled DS pair at a high bias field of 290 V/mm [Fig. 2(c)]. These intensity patterns of each beam were taken immediately after blocking the pairing beam. In contrast, Fig. 2(d) shows that, after the pairing beam was removed and the remaining beam reached a new steady state, each beam itself

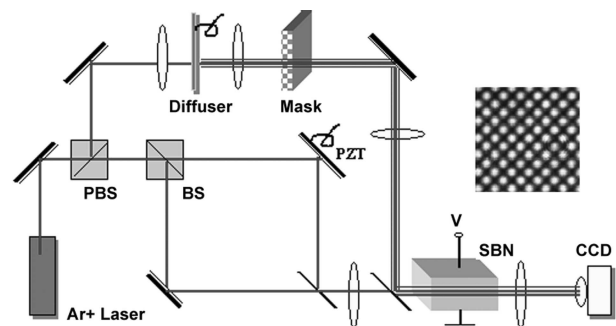


Fig. 1. Experimental setup: PBS, polarizing beam splitter; BS, beam splitter; PZT, piezoelectric transducer; SBN, strontium barium niobate; V, voltage. Inset, photonic lattice created by optical induction.

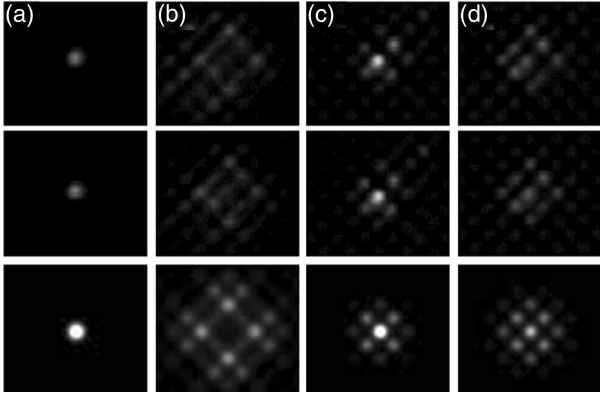


Fig. 2. Experimental and numerical results of a 2D discrete vector soliton. (a) Input, (b) discrete diffraction at low bias field, (c) mutual trapping, (d) decoupled output at high bias field. Rows 1 and 2 show the two components of the vector soliton from the experiment. Since the two components from the simulations are the same, only the  $U$  component is shown (row 3).

no longer formed a DS under the same conditions. These results illustrate that the observed vector soliton in Fig. 2(c) arises from mutual trapping of two nonlinearly interacting beams in the lattice, and the soliton structure is not possible should one of the components be absent. As in the case of a scalar lattice soliton,<sup>5–8</sup> a vector lattice soliton requires a balance between the waveguide coupling offered by the lattice and the self-focusing nonlinearity controlled by the combined intensity of both beams (when other experimental parameters are unchanged). Thus, after removing one beam, the balance cannot be maintained and the other beam experiences only partial focusing [Fig. 2(d)]. When the two beams were recombined, the vector soliton was reformed in a steady state. Without the lattice the two beams could not form a coupled soliton pair under these experimental conditions, although such a soliton pair has been observed before in a different nonlinear regime.<sup>17</sup>

The above experimental results were also observed in our numerical simulations of the coupled 2D nonlinear wave equations with a periodic lattice potential. The nondimensional model for propagation of two mutually incoherent beams in a lattice can be expressed as<sup>5,6</sup>

$$i \frac{\partial U}{\partial z} + \frac{\partial^2 U}{\partial x^2} + \frac{\partial^2 U}{\partial y^2} - \frac{E_0}{1 + I(x, y) + |U|^2 + |V|^2} U = 0, \quad (1)$$

$$i \frac{\partial V}{\partial z} + \frac{\partial^2 V}{\partial x^2} + \frac{\partial^2 V}{\partial y^2} - \frac{E_0}{1 + I(x, y) + |U|^2 + |V|^2} V = 0, \quad (2)$$

where  $I = I_0 \sin^2[(x + y)/\sqrt{2}] \sin^2[(x - y)/\sqrt{2}]$ ;  $U$  and  $V$  are the slowly varying amplitudes of the two beams normalized by the square root of the dark irradiance of the crystal  $I_d$ ;  $z$  is the distance along the direction of the crystal (measured in units of  $2k_1 D^2/\pi^2$ );  $x$  and  $y$  are distances along the transverse directions (measured in units of  $D/\pi$ );  $I_0$  is the peak intensity

of the photonic lattice normalized by  $I_d$ ;  $E_0$  is the applied dc field [measured in units of  $\pi^2/(k_0^2 n_e^4 D^2 r_{22})$ ];  $D$  is the lattice spacing;  $k_0 = 2\pi/\lambda_0$  is the wave number;  $k_1 = k_0 n_e$ ; and  $n_e$  and  $r_{33}$  are the unperturbed refractive index and the electro-optic coefficient for the extraordinarily polarized beam, respectively. As in the experiment, we chose parameters as  $D = 20 \mu\text{m}$ ,  $\lambda_0 = 0.5 \mu\text{m}$ ,  $n_e = 2.3$ ,  $r_{33} = 280 \text{ pm/V}$ , and  $I_0 = 3I_d$ . Thus in our simulation one  $x$  or  $y$  unit corresponds to  $6.4 \mu\text{m}$ , one  $z$  unit corresponds to  $2.3 \text{ mm}$ , and one  $E_0$  unit corresponds to  $20 \text{ V/mm}$  in physical units. The initial conditions for  $U$  and  $V$  are Gaussian beams centered at the same lattice site, with equal peak intensity. Their combined intensity is  $1/5$  of the lattice intensity, and their FWHMs are  $10 \mu\text{m}$ . Numerical results after  $15 \text{ mm}$  of propagation are shown in the bottom row of Fig. 2, where Fig. 2(a) shows the input, Fig. 2(b) shows the discrete diffraction at  $E_0 = 50 \text{ V/mm}$ , and Figs. 2(c) and 2(d) show the coupled and decoupled components, respectively, of a lattice vector soliton at  $E_0 = 140 \text{ V/mm}$ . Since the two components are exactly the same, only the  $U$  component is shown. These results are in good agreement with our experimental observations.

The above results suggest the existence of fundamental vector solitons in model Eqs. (1) and (2). We show that this is indeed the case. In fact, because of the rotational symmetry of the equations, a fundamental vector soliton can be obtained from scalar solitons as  $U = \phi(x, y) \cos \theta \exp(-i\mu z)$ ,  $V = \phi(x, y) \sin \theta \times \exp(-i\mu z)$ , where  $\phi(x, y)$  is the scalar lattice soliton satisfying

$$\frac{\partial^2 \phi}{\partial x^2} + \frac{\partial^2 \phi}{\partial y^2} + \mu \phi - \frac{E_0}{1 + I(x, y) + \phi^2} \phi = 0, \quad (3)$$

$\theta$  is an arbitrary projection angle, and  $\mu$  is the propagation constant. Scalar lattice solitons were studied in Refs. 5, 6, and 11. To further understand these solitons and their stability behaviors, we obtained them numerically from Eq. (3) by relaxation methods. The results at  $E_0 = 140 \text{ V/mm}$  are shown in Fig. 3, where Fig. 3(a) is the lattice field and Figs. 3(b) and 3(c) are the scalar lattice soliton obtained with different peak intensities. The lattice soliton is localized at moderate intensities and spreads to more lattice sites at low intensities. Figure 3(d) illustrates the non-dimensional power and peak intensity diagrams versus propagation constant  $\mu$ , which shows that there is a minimal power below which lattice solitons cannot exist. Suggested by the Vakhitov and Kolokolov stability

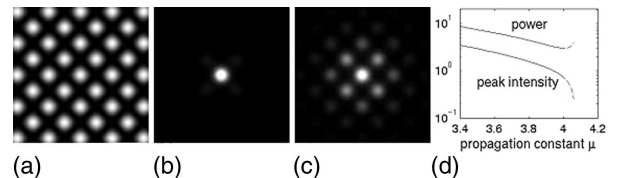


Fig. 3. Exact solutions of scalar lattice solitons at  $E_0 = 140 \text{ V/mm}$  and  $I_0 = 3I_d$ . (a) Lattice pattern, (b) more localized soliton (with peak intensity  $I = I_d$ ), (c) less localized soliton (with peak intensity  $I = I_d/4$ ), (d) normalized power and intensity diagram.

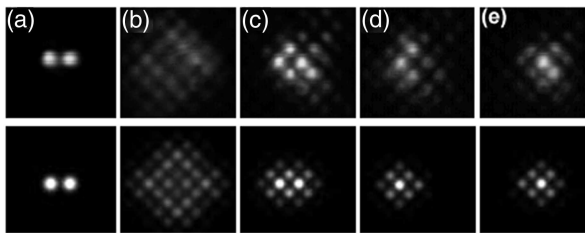


Fig. 4. Demonstration of dipolelike vector solitons in a 2D lattice. Top, experimental results. Bottom, corresponding numerical results. (a) Combined input; (b) and (c) combined output at low- and high-bias fields, respectively; (d), (e)  $U$  and  $V$  components from (c).

criterion,<sup>18</sup> lattice solitons on the right (left) side of this minimal-power point are linearly unstable (stable). We have confirmed this by directly simulating the linearized equation around scalar solitons. A similar finding for the case of Kerr nonlinearity was reported in Ref. 11.

When the two mutually incoherent beams are launched in parallel into two neighboring lattice sites rather than overlapped into one site, a dipolelike vector soliton is observed. The experimental results are shown in Fig. 4 (top row). The initial spacing between the two beams is  $\sim 28 \mu\text{m}$  to match the two diagonal lattice sites [Fig. 4(a)]. At a low bias of 90 V/mm the combined pattern covers several lattice sites at crystal output due to discrete diffraction [Fig. 4(b)]. As the field is increased to 320 V/mm, the two beams are trapped into mainly the two input lattice sites, but a significant portion of the energy remains in the two orthogonal lattice sites [Fig. 4(c)]. When each beam is viewed separately, a localized but asymmetric pattern is observed [Figs. 4(d) and 4(e)] in which mutual coupling between the left and the right beams is visible. Without the lattice, mutually incoherent soliton beams tend to attract each other at such close proximity.

Numerically, we simulated the evolution of a dipolelike vector soliton in Eqs. (1) and (2) corresponding to our experiments. The results for a simulation distance of 15 mm are shown in Fig. 4 (bottom panel), where Fig. 4(a) is the input; Figs. 4(b) and 4(c) are the combined output at bias fields of 50 and 140 V/mm, respectively; and Figs. 4(d) and 4(e) are the  $|U|$  and  $|V|$  components, respectively, of Fig. 4(c). These results qualitatively resemble those from the experiments. In particular, in addition to the satellite lobes developed at the four sides of the main beam, which is typical of scalar lattice solitons, there is another lobe in each component that overlaps with the main beam in the other component. This additional lobe (as also seen in our experiment) is due to the nonlinear coupling between the two components. Without the coupling this lobe would not exist, and the DS would have a symmetric intensity pattern. The slight difference between intensity patterns obtained from experiment and simulation might be attributed to diffusion-induced self-bending effects,<sup>17</sup> which were not included in our model for simplicity.

On the basis of the above results, one may wonder whether the exact solutions for dipolelike vector solitons exist in the theoretical model of Eqs. (1) and (2). As seen in Figs. 4(d) and 4(e), such solitons should have an asymmetric intensity pattern in each component. We searched for such solitons extensively by use of the relaxation methods but were not able to find any. We note, however, that the exact solutions for single-component dipole solitons in a lattice do exist.<sup>19</sup>

In summary, we have demonstrated the formation of 2D vector solitons in an optically induced photonic lattice. We expect these solitons to be found in other relevant periodic nonlinear systems.

This work was supported in part by the U.S. Air Force Office of Scientific Research, the NASA Experimental Program to Stimulate Competitive Research, Research Corp., and the National Natural Science Foundation of China. Z. Chen's e-mail address is zchen@stars.sfsu.edu.

## References

1. D. N. Christodoulides, F. Lederer, and Y. Silberberg, *Nature* **424**, 817 (2003).
2. D. Campbell, S. Flach, and Y. S. Kivshar, *Phys. Today* **57**(1), 43 (2004).
3. H. S. Eisenberg, Y. Silberberg, R. Morandotti, A. R. Boyd, and J. S. Aitchison, *Phys. Rev. Lett.* **81**, 3383 (1998).
4. R. Morandotti, H. S. Eisenberg, Y. Silberberg, M. Sorel, and J. S. Aitchison, *Phys. Rev. Lett.* **86**, 3296 (2001).
5. J. W. Fleischer, T. Carmon, M. Segev, N. K. Efremidis, and D. N. Christodoulides, *Phys. Rev. Lett.* **90**, 023902 (2003).
6. J. W. Fleischer, T. Carmon, M. Segev, N. K. Efremidis, and D. N. Christodoulides, *Nature* **422**, 150 (2003).
7. D. Neshev, E. Ostrovskaya, Y. Kivshar, and W. Krolikowski, *Opt. Lett.* **28**, 710 (2003).
8. H. Martin, E. D. Eugenieva, Z. Chen, and D. N. Christodoulides, *Phys. Rev. Lett.* **92**, 123902 (2004).
9. Z. Chen, H. Martin, E. D. Eugenieva, J. Xu, and A. Bezryadina, *Phys. Rev. Lett.* **92**, 143902 (2004).
10. B. A. Malomed and P. G. Kevrekidis, *Phys. Rev. E* **64**, 026601 (2001).
11. J. Yang and Z. H. Musslimani, *Opt. Lett.* **28**, 2094 (2003).
12. F. Lederer, S. Darmanyan, and A. Kobaykov, in *Spatial Optical Solitons*, S. Trillo and W. E. Torruellas, eds. (Springer-Verlag, New York, 2001).
13. M. J. Ablowitz and Z. H. Musslimani, *Phys. Rev. E* **65**, 056618 (2002).
14. J. Hudock, P. G. Kevrekidis, B. A. Malomed, and D. N. Christodoulides, *Phys. Rev. E* **67**, 056618 (2003).
15. J. Meier, J. Hudock, D. N. Christodoulides, G. Stegeman, Y. Silberberg, R. Morandotti, and J. S. Aitchison, *Phys. Rev. Lett.* **91**, 143907 (2003).
16. Z. Chen and K. McCarthy, *Opt. Lett.* **27**, 2019 (2002).
17. Z. Chen, M. Segev, T. H. Coskun, and D. N. Christodoulides, *Opt. Lett.* **21**, 1436 (1996).
18. N. G. Vakhitov and A. A. Kolokolov, *Radiophys. Quantum Electron.* **16**, 783 (1973).
19. J. Yang, I. Makasyuk, A. Bezryadina, and Z. Chen, *Opt. Lett.* **29**, 1662 (2004).